Title Page

Seasonal growth and senescence of seagrass alters sediment accumulation rates and carbon burial in a coastal lagoon

Qingguang Zhu[1], Patricia L. Wiberg[1], Karen J. McGlathery[1]

[1]Department of Environmental Sciences, University of Virginia, Charlottesville, VA, USA

Corresponding author: Qingguang Zhu (qz3cp@virginia.edu), ORCID 0000-0002-0915-8280

Running head: seasonal sediment accumulation in seagrass beds

Keywords: sediment transport, carbon burial, seasonal variation, flow-vegetation interactions, numerical modeling, seagrass meadows

Abstract

Seagrass meadows are important carbon sinks in the global coastal carbon cycle yet are also among the most rapidly declining marine habitats. Their ability to sequester carbon depends on flow-sediment-vegetation interactions that facilitate net deposition, as well as high rates of primary production. However, the effects of seasonal and episodic variations in seagrass density on net sediment and carbon accumulation have not been well quantified. Understanding these dynamics provides insight into how carbon accumulation in seagrass meadows responds to disturbance events and climate change. Here we apply a spatially resolved sediment transport model that includes coupling of seagrass effects on flow, waves, and sediment resuspension in a seagrass meadow to quantify seasonal rates of sediment and carbon accumulation in the meadow. Our results show that organic carbon accumulation rates were largely determined by sediment accumulation and that they both changed non-linearly as a function of seagrass shoot density. While seagrass meadows effectively trapped sediment at meadow edges during spring-summer growth seasons, during winter senescence low-density meadows (< 160 shoots m^{-2}) were erosional with rates sensitive to density. Small variations in winter densities resulted in large changes in annual sediment and carbon accumulation in the meadow; meadow-scale (hundreds of square meters) summer seagrass dieback due to marine heatwaves can result in annual erosion and carbon loss. Our findings highlight the strong temporal and spatial variability in sediment accumulation within seagrass meadows and the implications for annual sediment carbon burial rates and the resilience of seagrass carbon stocks under future climate change.

Introduction

Seagrass meadows are essential coastal habitats that offer valuable ecosystem services including carbon sequestration, nutrient cycling and improved water quality, and sediment stabilization (de Boer 2007; McGlathery et al. 2007). They have been recognized as important carbon sinks in the global marine carbon cycle due to high rates of net primary production and carbon burial in the sediment (Duarte et al. 2013), and contribute to more than 10% of the annual sediment carbon burial in global oceans (Fourqurean et al. 2012). Despite their importance in coastal ecosystems, seagrasses are one of the most rapidly declining marine habitats, threatened by degraded water quality, temperature stress, and sea level rise (Orth et al. 2006; Waycott et al. 2009). The disappearance of seagrass can cause seabed erosion and the exposure of accumulated sediment carbon to oxic conditions, leading to carbon emissions (Pendleton et al. 2012; Aoki et al. 2021). For seagrass meadows to be considered as effective carbon sinks, the accumulated carbon must be preserved in sediments for a long period (e.g., decades to centuries).

An accurate estimate of sediment accumulation rates within seagrass meadows is critical for quantifying sediment budgets and organic carbon burial. Various methods have been used to determine sediment accumulation rates in seagrass meadows worldwide, each focusing on different temporal scales and spatial extents (Potouroglou et al. 2017). Repeated bathymetric surveys can provide a direct measure of long-term changes in deposition at large spatial scales (Walter et al. 2020), but lack the precision to capture most short-term change (e.g., annual or seasonal scale). Radiometric dating methods are widely used in seagrass studies to determine sedimentation rates over several decades (Duarte et al. 2013), but they have been criticized for not accounting for surface mixing effects (Johannessen and Macdonald 2016). Sediment traps/plates are able to measure sediment deposition over a period of several days to months, but they cannot fully resolve erosion/resuspension processes on the seabed and the results are susceptible to sediment loss during retrieval (Gacia and Duarte 2001; Nolte et al. 2013). Surface elevation tables can provide precise short-term and long-term measurements, but are limited in spatial scale and may cause local scouring of the seabed (Potouroglou et al. 2017).

Long-term sediment accumulation rates within seagrass meadows have been characterized at a number of sites using the aforementioned approaches (Greiner et al. 2013; Duarte et al. 2013; Oreska et al. 2020), but short-term dynamics of sediment accumulation in seagrass meadows remain unclear. Seagrass beds show strong temporal and spatial variability in erosion and deposition in response to seasonal seagrass growth and senescence (Hansen and Reidenbach 2013; Zhu et al. 2021) that is difficult to interpret from long-term sedimentary records. There is also growing evidence of increasing frequency of marine heatwaves that can cause seasonal summer seagrass dieback and losses of accumulated carbon in seagrass sediments (Arias-Ortiz et al. 2018; Aoki et al. 2021). Because these short-term processes and disturbances can strongly alter annual sediment budgets and long-term dynamics of seagrass meadows, it is important to understand these seasonal sediment dynamics and the associated drivers, especially in the context of future climate change.

An alternative approach to characterizing sediment accumulation rates in seagrass meadows is through modeling. Numerical models capable of resolving the synergistic effects of flow-wave-vegetation-sediment interaction (Chen et al. 2007; Carr et al. 2016; Donatelli et al. 2018) provide a tool for understanding seasonal sediment dynamics in seagrass meadows in spatially resolved settings. However, most previous modeling studies of sediment transport within seagrass meadows have used idealized seagrass meadows or did not resolve seasonal seagrass growth and wind patterns. To better resolve spatial variations of dynamic factors and to understand the effects of seasonal growth of seagrass on sediment accumulation, we applied the process-based hydrodynamic and sediment transport Delft3D model, including coupling of seagrass effects on flow, waves, and sediment resuspension, to a seagrass meadow in a shallow coastal bay in Virginia, USA. The model has been parameterized and extensively validated using long-term data from the site (wind conditions, hydrodynamic and suspended sediment data, sediment accumulation rates, and seagrass characteristics; Zhu et al. 2021).

In this study, the coupled model was run for 12 consecutive months with seasonally varying winds and tides as well as seagrass densities. The results were analyzed to address three questions. (1) How do rates of sediment accumulation and organic carbon burial within seagrass meadows vary in response to seasonal variations in seagrass density? (2) How does short-term disturbance in seagrass density affect annual sediment accumulation rates? (3) What are the effects of seasonal variations in seagrass density on spatial sediment erosion/deposition patterns in seagrass meadows?

Study site

The study site, South Bay, is one of the back-barrier bays within the Virginia Coast Reserve Long-Term Ecological Research site (Fig. 1a). It is bordered by a barrier island to the east and is connected to two tidal inlets that exchange water with the Atlantic Ocean (Fig. 1b). South Bay has a mean depth of 1 m below mean sea level and an average semidiurnal tidal range of 1.2 m (Fagherazzi and Wiberg 2009). Sea level in the study area is rising at a rate of 4-5 mm yr^{-1} (https://tidesandcurrents.noaa.gov/sltrends/sltrends_station.shtml?id=8631044). South Bay is a shallow, oligotrophic environment that provides favorable light conditions for seagrass growth and is a successful seagrass restoration site where *Zostera marina* now dominates the subtidal flats (McGlathery et al. 2012). Located at the southern geographical limit for *Zostera marina* growth in the Western Atlantic Ocean (Aoki et al. 2020), the seagrass meadows in South Bay show strong seasonal variability that significantly impacts bay dynamics (Hansen and Reidenbach 2013; Rheuban et al. 2014). Seagrasses within the bay reach a maximum shoot density (> 500 shoots m^{-2}) in early summer and suffer from a mid-season loss due to heat stress in late summer; the density slightly increases in autumn after temperatures moderate and then declines to a minimum (50-100 shoots m^{-2}) during winter senescence. When the temperature increases in the next spring, seagrasses start to re-grow and the density gradually increases to 300 shoots m^{-2} in late spring (Fig. 1c; Hansen and Reidenbach 2013; Rheuban et al. 2014; Reidenbach and Thomas 2018; Berger et al. 2020). The presence of high-density seagrass significantly reduces sediment resuspension within seagrass meadows during summer, while significant sediment resuspension occurs in winter when frequent and stronger northeasterly winds coincide with minimum seagrass density (Hansen and Reidenbach 2013; Zhu et al. 2021).

Overall, seagrass meadows in South Bay effectively accumulate fine particles with an average sediment deposition rate of 6.3 mm yr^{-1} (based on radiometric dating at two representative sites; Greiner et al. 2013; Oreska et al. 2018), and resulted in a finer sediment grain size (mean = 71 μm) within the meadow than outside the meadow (mean = 124 μm; Lawson et al. 2007; McGlathery et al. 2012; Oreska et al. 2017). As a result of sediment accumulation, the seagrass meadow is able to bury organic carbon at an average rate of 42 g C m^{-2} yr^{-1} (Oreska et al. 2020).

Methods

Hydrodynamic and sediment transport simulations were conducted using the process-based and spatially resolved Delft3D FLOW/MOR model (Lesser et al. 2004), coupled with the nearshore phase-averaged wave model SWAN (Booij et al. 1999). The domain decomposition technique (Deltares 2014) was used to locally refine the model grid in South Bay to better capture seagrass meadows in the bay and the bordering barrier island. The model grid consisted of a small model domain covering the core study area in South Bay (Fig 1b; 305 × 302 grid cells with a spatial resolution of ~70 m) and a large model domain spanning the rest of the Virginia Coast Reserve (148 × 444 grid cells with a spatial resolution of 200 m). The open ocean boundaries of the large model domain were forced with water levels extracted from the NOAA tide gauge station at Wachapreague (Site ID:8631044) after adjusting tidal amplitude and phase to generate tidal simulation results in excellent agreement with measured tides at Wachapreague ($R^2 \geq 0.98$ and root mean square error ≤ 0.07 m). Wave simulations were driven by hourly wind conditions from the same NOAA station and coupled with the flow model every hour. Model bathymetry and bottom sediment size distributions and properties were extracted from Wiberg et al. (2015). Three sediment classes were used in the model: a 32-64 μm coarse silt fraction, a < 32 μm medium to fine silt fraction, and a > 64 μm sand fraction (a representative median grain size of 125 μm was defined in the model for the sand fraction). To better capture the effects of seagrass on sediment transport, sediment size distributions in the South Bay seagrass meadows were initialized based on local surveys from Oreska et al. (2017). The active sediment layer thickness, which defines the maximum erosion depth of the seabed at each model time step, was set to 5 cm to avoid unrealistically high sediment availability.

The model was implemented in depth-averaged mode with a time step of 0.25 min. Several previous studies have shown that depth-averaged Delft3D simulations are able to produce reasonable results for well-mixed shallow coastal bays, including the Virginia Coast Reserve, and to resolve the synergistic effects of flow-wave-vegetation-sediment interactions in spatially resolved settings (Nardin and Edmonds 2014; Nardin et al. 2018; Zhu et al. 2021). In order to incorporate seagrass effects on currents and waves, the Baptist vegetation model (Baptist et al. 2007) and the Suzuki vegetation wave energy dissipation model (Suzuki et al. 2012) were implemented in the Delft3D FLOW module and the SWAN model, respectively. These two methods considered vegetation as cylindrical structures characterized by vegetation height, stem diameter, shoot density, and vegetation flow drag coefficient and wave drag coefficient (Table S1).

The coupled model has been parameterized and extensively validated using summer and winter hydrodynamic and suspended sediment data during a 4-day period in January and June 2011 from a seagrass site and a nearby unvegetated site in South Bay (Zhu et al. 2021). Model skill indices, including bias, root mean square error, and Willmott skill index (Willmott 1981), were calculated for model validation parameters (water level, significant wave height, depth-averaged velocity, and total suspended sediment concentration) to quantify model ability to characterize hydrodynamic and suspended sediment characteristics in the bay. Values of the Willmont skill index are summarized in Table S2. Excellent agreement between modeled and measured water levels was obtained at both sites during each validation period. Wave height skill scores (0.56-0.87) for the seagrass site were generally higher than those of the unvegetated site. While generally good agreement between modeled and measured depth-averaged velocity was obtained at both sites, the model slightly over-estimated peak velocity during flood tides with an average bias of 0.05 m s^{-1} (Zhu et al. 2021). The model successfully captured most sediment resuspension events at both sites during winter (skill scores $\geq$ 0.80) and predicted a strong reduction of suspended sediment concentration (> 80%) in the summer seagrass meadow that is consistent with field observations. See Zhu et al. (2021) for further details of the model parameterization and validation. Overall, the coupled model is able to provide spatially-resolved simulations of flow and sediment transport patterns within/outside the seagrass meadow with performance similar to that of other model studies considering seagrass effects (Chen et al. 2007; Moki et al. 2020).

In this study, we extended the simulation period considered in Zhu et al. (2021) to a complete annual cycle using winds and tidal forcing for a representative year (August 1, 2011 to July 31, 2012; Fig. S1), with typical seasonal seagrass characteristics (shoot density ranging from 100-600 shoots m^{-2}, seagrass height ranging from 0.2-0.4 m, and stem diameter ranging from 0.2-0.4 cm) observed from the site (Table S1). Evaluating model sensitivity to variations in seagrass characteristics, Zhu et al. (2021) found that variations in seagrass shoot density had a larger impact on bay dynamics than did variations in seagrass height and stem diameter. Considering the wide range of annual seagrass density variation (100-600 shoots m^{-2}) and its strong impact on bay dynamics at our study site, we mainly focused on the impacts of seagrass density variations in this paper.

In order to better represent observed spatial density gradients in the meadow, three seagrass density classes were assigned in the model each month, with the highest density (N) in the central meadow, an intermediate density of $0.8N$ outside the central area, and the lowest density of $0.6N$ near meadow edges (Fig. 1b). A reference model case without seagrass was also run for the same simulation period for comparison. The model was run for a three-month spin-up period to reach a quasi-equilibrium state prior to beginning the annual simulations, and results generated during the spin-up run were used as initial conditions for the annual simulations to avoid disturbances caused by model initialization.

The coupled model is able to simulate mineral sediment transport processes but cannot explicitly simulate organic carbon sequestration. In order to quantify organic carbon burial rates in the meadow, a negative linear relationship between sediment organic carbon concentration and sand fraction was established (Fig. S2; $R^2 = 0.75$) based on previous measurements from Oreska et al. (2017) within the same meadow. Using this relationship, monthly distributions of sand fraction (Fig. S3) output from model simulations were converted to maps of surface sediment organic carbon concentration (Fig. S4). Then monthly distributions of organic carbon burial rate [mg month^{-1} cm^{-2}] in the meadow (Fig. S5) were determined by multiplying modeled sediment accumulation rates [mm month^{-1}] by the surface sediment organic carbon concentration [mg cm^{-3}].

Results

Sediment and organic carbon accumulation rates vary with seagrass density

With seasonally varying seagrass densities, our simulation results show that bed shear stress and total suspended sediment concentration averaged across the seagrass meadow changed non-linearly as a function of seagrass density (Fig. 2a, 2b). The most rapid changes of bed shear stress and total suspended sediment concentration occurred at low seagrass densities, while there was little change in bed shear stress and total suspended sediment concentration when seagrass densities were > 200 shoots m^{-2}. Throughout the year, sediment resuspension in the meadow was mainly controlled by seagrass density rather than wind speeds (Fig. S6).

Similarly, seasonal growth and senescence of seagrass exerted a strong influence on sediment accumulation and carbon burial within seagrass meadows. Four low-density scenarios (seagrass shoot density N = 0, 25, 50 and 100 shoots m^{-2}) were specified during winter conditions to better resolve the effects of low seagrass density (Table S1). Simulation results show that rates of sediment accumulation and organic carbon burial averaged across the meadow varied strongly with seagrass density (Fig. 2c, 2d). When seagrass density was lower than 160 shoots m^{-2}, typical in winter, seagrass beds were erosional with rates that were sensitive to density. When seagrass density > 200 shoots m^{-2}, rates of sediment accumulation and organic carbon burial were relatively constant due to strong flow retardation (Fig. 2c, 2d, and S7). At the meadow scale the average organic carbon accumulation rate was largely determined by sediment accumulation (Fig. 3; $R^2 = 0.99$). On the annual time scale, simulations with typical seasonal seagrass characteristics predicted a meadow-averaged sediment accumulation rate of 4.1 ± 0.5 (standard error) mm yr^{-1} and a carbon accumulation rate of 22 ± 1.6 (standard error) g C m^{-2} yr^{-1}.

Based on model results showing how monthly sediment accumulation rates vary as a function of seagrass density (Fig. 2c), we can design density variation scenarios by changing the seagrass density in specific months and quantifying the corresponding effect (e.g., short-term winter density variations and summer seagrass dieback due to marine heatwaves) on annual sediment accumulation rates. Three density variation scenarios were constructed: lower-than-average winter density (winter seagrass density reduced by 50 shoots m^{-2}); higher-than-average winter density (winter seagrass density increased by 50 shoots m^{-2}); and a summer marine heatwave scenario with summer seagrass density reduced to 50 shoots m^{-2} (Aoki et al. 2021). For the lower-than-average winter density scenario, sediment accumulation rates in winter months were much lower than in the normal-density simulations (red symbols in Fig. 2e) and the annual sediment accumulation rate was reduced by 44% to 2.3 mm yr^{-1}. For the higher-than-average winter density scenario, the seagrass meadow accumulated sediment during the entire winter (gray symbols in Fig. 2e), resulting in an annual sediment accumulation rate of 6.6 mm yr^{-1}, a 61% increase compared with the rate under typical densities. For the summer marine heatwave scenario, the meadow became erosional, with an annual sediment accumulation rate of -1.0 mm

yr^{-1} (Fig. 2f), thereby leading to the release of stored carbon in seagrass sediments (-4.6 g C m^{-2} yr^{-1}). This modeling result of seabed erosion and sediment carbon loss is in general agreement with a previous study in the same meadow documenting a net loss of 20% of sediment carbon in the upper 5 cm of the bed (not including the effects of bed level changes) caused by a summer marine heatwave in 2015 (Aoki et al. 2021).

Spatial erosion and deposition pattern within meadows

To better understand the spatial variability of seasonal sediment accumulation at the meadow scale, we divided our annual simulation results into four groups according to the seagrass growth cycle at our study site: summer growth and mid-season loss from June to August, autumn regrowth from September to October, winter senescence from November to March, and early growth from April to May. Our simulation results show that there were strong spatial gradients of bed shear stress from the meadow edge toward the interior (Fig. S8), and these spatial gradients had a significant impact on seasonal erosion/deposition patterns. Sediment accumulation mainly occurred at meadow edges during summer when seagrass density was high (Fig. 4a) and decreased rapidly with distance into the meadow interior (Fig. 4e). When seagrass density decreased in autumn, the meadow still accumulated sediment with a lower deposition rate, and this sediment could be transported further into the meadow interior due to weaker flow attenuation by the seagrass (Fig. 4b, S8b). During the minimum densities in winter, most of the meadow experienced erosion (Fig. 4c). The most severe erosion occurred near meadow edges during the winter senescence period (~9 mm), an amount roughly equal to the mass of sediment deposited at the edges in summer (Fig. 4e). When seagrass started regrowing in spring, the meadow once again became depositional, with sediment accumulating at meadow edges, but at lower rates compared to the summer growing season (Fig. 4d). Seasonal organic carbon accumulation patterns were similar to those for sediment accumulation (Fig. S5).

On the annual time scale, the meadow-averaged sediment accumulation rate was low (0.4 ± 0.2 mm yr^{-1}) in the simulation with no seagrass, whereas the presence of a seagrass meadow maintained a higher average sediment accumulation rate of 4.1 ± 0.5 mm yr^{-1} (Fig. 5a, 5b). Despite the large spatial variability of sediment accumulation rates across the meadow (Fig. 5d), the modeled sediment accumulation rates agreed reasonably well with rates estimated from ^{210}Pb dating in previous studies at two sites of the meadow (see locations in Fig. 5b); the modeled sediment accumulation rates at the central and northern sites were 5.0 and 4.3 mm yr^{-1}, respectively, while the rates estimated from ^{210}Pb dating were 6.6 and 6.0 mm yr^{-1} at these two sites (Greiner et al. 2013; Oreska et al. 2018). Pronounced sediment accumulation (> 4.0 mm yr^{-1}) occurred at meadow edges and in the northwestern and southern portion of the meadow interior (Fig. 5b), in good agreement with previous observations from Oreska et al. (2017) within the same meadow. Because the amount of sediment accumulation at meadow edges in summer was largely offset by winter erosion (Fig. 4e), the annual sediment accumulation rate near the edge was mainly dependent on deposition during autumn regrowth and spring early growth seasons. During autumn regrowth, winter senescence, and early growth seasons, sediment could be transported further into the northwestern and southern portion of the meadow (Fig. 4) where larger water depths resulted in lower bed shear stress and promoted sediment accumulation (Fig. 5b, 5c). At the meadow scale, while there was no depth preference for sediment erosion/deposition in simulations without seagrass effects (Fig. 6a), deeper locations within the meadow tended to receive more sediment deposition than shallow ones when seagrass effects were included in model simulations (Fig. 6b).

Discussion and conclusions

A number of field studies (Hasegawa et al. 2008; Hansen and Reidenbach 2013) have shown that high densities of seagrass in the summer growing season resulted in larger reductions in bed shear stress and sediment resuspension compared with low-density meadows in winter. However, the effects of seasonally varying seagrass densities on sediment accumulation have not been well quantified due to the lack of monthly or seasonal measurements. Our annual simulation results show that sediment accumulation rates within seagrass meadows changed non-linearly between seasons as a function of seagrass density (Fig. 2c). The most rapid changes of sediment accumulation rates occurred at low seagrass densities in winter (Fig. 2c), while there was little change in sediment accumulation rates when seagrass densities were > 200 shoots m^{-2} during other seasons due to effects of strong flow reduction at high shoot densities (Fig. 2a, S7; Hansen and Reidenbach 2013).

Our seagrass density variation scenarios show that small variations in winter shoot density can result in large changes (> 40%) in annual sediment accumulation rates of the meadow (Fig. 2e). Considering that most previous research has focused on flow and sediment dynamics in high-density meadows (Donatelli et al. 2018), more comprehensive investigations of sediment accumulation during low-density seasons are needed to better resolve the effects of seagrass density variations on annual sediment accumulation. We also found that summer seagrass dieback events, for example due to marine heatwaves, can change seagrass beds from depositional (4.1 mm yr^{-1}) to erosional (-1.0 mm yr^{-1}; Fig. 2f) on annual timescales. This strong sensitivity of sediment accumulation rates to seagrass density variations has significant implications for future scenarios of change. If seagrasses were present in much lower densities due to degradation, physical disturbance, or increasing frequency of marine heatwaves, meadows would inevitably become erosional and release accumulated carbon (Arias-Ortiz et al. 2018; Walter et al. 2020), like the observed sediment carbon loss associated with the 2015 summer marine heatwave in South Bay seagrass meadows (Aoki et al. 2021). Moreover, if seagrasses were exposed to multiple years of degraded environmental conditions, including temperature stress, the continuous erosion of seagrass beds associated with reduced seagrass growth would increase water depth of the bay and promote sediment resuspension, thereby creating a less favorable light condition for seagrass growth and potentially triggering irreversible collapse of meadows (Carr et al., 2012).

Although previous studies have shown that seagrasses can effectively trap sediment and promote sediment deposition (Gacia and Duarte 2001), there have been few direct meadow-scale observations of spatial erosion/deposition patterns within seagrass meadows. Very little is known about the spatial sediment deposition pattern in response to seasonal seagrass density variations. Our simulation results show that edge effects play an important role in seasonal patterns of sediment accumulation and carbon burial at a meadow scale (Fig. 4, S5). This is supported by spatial autoregressive analyses in the same meadow that found that edge proximity was more important than shoot density and meadow age in determining sediment organic carbon content (Oreska et al. 2017). Sediment accumulation mainly occurred at meadow edges in spring and summer growth seasons when seagrass density was relatively high (Fig. 4a, 4d). The modeled sediment accumulation at meadow edges in the present study was in good agreement with other model results considering seagrass edge effects at high shoot densities (Chen et al. 2007; Carr et al. 2016). During the winter senescence period, severe erosion (~9 mm) was observed near meadow edges, an amount roughly equal to 40%-50% of the mass of sediment deposited at the edges in other seasons (Fig. 4).

During autumn regrowth, winter senescence, and early growth seasons, lower densities of seagrass allow sediment to be advected further into the meadow (Fig. 4b, 4c, and 4d), providing the primary mechanism for sediment deposition in the interior of the meadow. Our simulation results show that water depth exerted a strong influence on the spatial pattern of sediment accumulation in the meadow interior (Fig. 6b). Together with edge effects, depth variations can produce strong spatial variability in sediment accumulation and carbon burial across the meadow (Fig. 5; Samper-Villarreal et al. 2016; Oreska et al. 2017). This has implications for site selection and timing of sediment sampling to characterize sediment accumulation and carbon burial in seagrass meadows. Ideally, sampling sites should include the meadow edge and interior, as well as deeper and shallower sites. Sampling during the autumn regrowth period may provide the best representation of the annual spatial pattern of deposition (Fig. 4b, 5b).

Organic carbon burial rates within the meadow were obtained by multiplying sediment accumulation rate by surface sediment organic carbon concentration at each model grid location. At the meadow scale, although there were spatial gradients of sediment organic carbon concentration from meadow edges to the interior (varying from 2 to 6 mg cm^{-3}; Fig. S4), the spatial pattern of organic carbon burial was largely determined by sediment accumulation (Fig. 3, Fig. 4 vs. Fig. S5) because of its strong spatial variability across the meadow (Fig. 5d). This is in agreement with a recent study indicating the strong impacts of sediment accumulation rates on organic carbon burial at a basin scale (Johannessen and Macdonald 2016). In some other systems where spatial distributions of sediment accumulation rate are relatively uniform, like those in lacustrine environments (Lin et al., 2022), the spatial pattern of organic carbon burial will more likely be controlled by spatial distributions of sediment organic carbon concentration.

On an annual time scale, our simulations with seasonal seagrass characteristics predicted a meadow-wide average sediment accumulation rate of 4.1 ± 0.5 mm yr^{-1}. This value is similar to the rapid rates of sea-level rise (4-5 mm yr^{-1}) at our study site, but is less than the average long-term sediment accumulation rate (6.3 mm yr^{-1}) determined by ^{210}Pb dating at two representative sites within the meadow (Greiner et al. 2013; Oreska et al. 2018). In future studies, more spatially distributed sediment accumulation rate measurements will be needed to constrain model simulation results and improve our understanding of spatial erosion/deposition patterns within seagrass meadows.

The modeled carbon accumulation rate averaged across the meadow (22 ± 1.6 g C m^{-2} yr^{-1}) was lower than the rate obtained from the meadow-scale carbon stock estimate in the same meadow based on 16 spatially distributed sampling sites (42 g C m^{-2} yr^{-1}; Oreska et al. 2020). The underestimation of sediment accumulation and carbon burial rates is likely due to the absence of primary production in model simulations. A more realistic approach would be to incorporate vegetation growth dynamics and organic matter trapping (e.g., Best et al. 2018; Brückner et al. 2019) into the coupled model. In addition, our model grid size (~70 m) was too coarse to resolve seagrass patchiness, which has been shown to play a significant role in distributions of bed shear stress and sediment accumulation (Ricart et al. 2015; Carr et al. 2016). Another limitation of this study is that we did not simulate temperature in the coupled model and therefore could not resolve the effects of biodegradation and mineralization on sediment carbon burial, which have been found to be important factors affecting carbon storage in other seagrass ecosystems (Sohma et al. 2018).

Our model was able to produce reasonable spatially-resolved simulations of sediment accumulation in seagrass meadows under seasonally varying winds and tides and seagrass densities. This is one of the first modeling attempts to examine in detail the extent and drivers of temporal and spatial variability in sediment accumulation and carbon burial within seagrass meadows. Our results have significant implications for seagrass ecosystems under future climate change. In a warming climate, seagrasses in temperate regions in the northern hemisphere will shift northward and the southernmost populations, like the meadows at our site, will likely face reduced growth and meadow loss due to temperature stress (Wilson and Lotze 2019). Marine heatwaves have already impacted seagrass meadows in this region (Berger et al. 2020; Aoki et al. 2021), and these are predicted to increase in frequency in future warming oceans (Oliver et al. 2019). Our modeling results of sediment accumulation in seagrass meadows and field studies from the same region (Aoki et al. 2021) indicate that under these circumstances, seabed erosion and carbon emissions will increase. Conservation actions are therefore urgently needed to mitigate the effects of climate change on seagrass ecosystems.

References

Aoki, L. R., K. J. McGlathery, P. L. Wiberg, and A. Al-Haj. 2020. Depth Affects Seagrass Restoration Success and Resilience to Marine Heat Wave Disturbance. Estuaries and Coasts **43**: 316–328. doi:10.1007/s12237-019-00685-0

Aoki, L. R., K. J. McGlathery, P. L. Wiberg, M. P. J. Oreska, A. C. Berger, P. Berg, and R. J. Orth. 2021. Seagrass Recovery Following Marine Heat Wave Influences Sediment Carbon Stocks. Front. Mar. Sci. **7**: 1170. doi:10.3389/fmars.2020.576784

Arias-Ortiz, A., O. Serrano, P. Masqué, and others. 2018. A marine heatwave drives massive losses from the world's largest seagrass carbon stocks. Nat. Clim. Chang. **8**: 1–7. doi:10.1038/s41558-018-0096-y

Baptist, M. J., V. Babovic, J. R. Uthurburu, M. Keijzer, R. E. Uittenbogaard, A. Mynett, and A. Verwey. 2007. On inducing equations for vegetation resistance. J. Hydraul. Res. **45**: 435–450. doi:10.1080/00221686.2007.9521778

Berger, A. C., P. Berg, K. J. McGlathery, and M. L. Delgard. 2020. Long-term trends and resilience of seagrass metabolism: A decadal aquatic eddy covariance study. Limnol. Oceanogr. **65**: 1423–1438. doi:10.1002/lno.11397

Best, S. N., M. Van der Wegen, J. Dijkstra, P. W. J. M. Willemsen, B. W. Borsje, and D. J. A. Roelvink. 2018. Do salt marshes survive sea level rise? Modelling wave action, morphodynamics and vegetation dynamics. Environ. Model. Softw. **109**: 152–166. doi:10.1016/j.envsoft.2018.08.004

Booij, N., R. C. Ris, and L. H. Holthuijsen. 1999. A third-generation wave model for coastal regions 1. Model description and validation. J. Geophys. Res. Ocean. **104**: 7649–7666. doi:10.1029/98JC02622

Brückner, M. Z. M., C. Schwarz, W. M. Dijk, M. Oorschot, H. Douma, and M. G. Kleinhans. 2019. Salt Marsh Establishment and Eco-Engineering Effects in Dynamic Estuaries Determined by Species Growth and Mortality. J. Geophys. Res. Earth Surf. **124**: 2962–2986. doi:10.1029/2019JF005092

Carr, J. A., P. D'Odorico, K. J. McGlathery, and P. L. Wiberg. 2012. Stability and resilience of seagrass meadows to seasonal and interannual dynamics and environmental stress. J. Geophys. Res. Biogeosci. **117**: 1007. doi:10.1029/2011JG001744

Carr, J. A., P. D'Odorico, K. J. McGlathery, and P. L. Wiberg. 2016. Spatially explicit feedbacks between seagrass meadow structure, sediment and light: Habitat suitability for seagrass growth. Adv. Water Resour. **93**: 315–325. doi:10.1016/j.advwatres.2015.09.001

Chen, S. N., L. P. Sanford, E. W. Koch, F. Shi, and E. W. North. 2007. A nearshore model to investigate the effects of seagrass bed geometry on wave attenuation and suspended sediment transport. Estuaries and Coasts **30**: 296–310. doi:10.1007/BF02700172

Deltares. 2014. Delft3D-FLOW User Manual (Version: 3.15.34158): Simulation of multi-dimensional hydrodynamic flows and transport phenomena, including sediments.

de Boer, W. F. 2007. Seagrass-sediment interactions, positive feedbacks and critical thresholds for occurrence: A review. Hydrobiologia **591**: 5–24. doi:10.1007/s10750-007-0780-9

Donatelli, C., N. K. Ganju, S. Fagherazzi, and N. Leonardi. 2018. Seagrass Impact on Sediment Exchange Between Tidal Flats and Salt Marsh, and The Sediment Budget of Shallow Bays. Geophys. Res. Lett. **45**: 4933–4943. doi:10.1029/2018GL078056

Duarte, C. M., H. Kennedy, N. Marbà, and I. Hendriks. 2013. Assessing the capacity of seagrass meadows for carbon burial: Current limitations and future strategies. Ocean Coast. Manag. **83**: 32–38. doi:10.1016/j.ocecoaman.2011.09.001

Fagherazzi, S., and P. L. Wiberg. 2009. Importance of wind conditions, fetch, and water levels on wave-generated shear stresses in shallow intertidal basins. J. Geophys. Res. **114**: F03022. doi:10.1029/2008JF001139

Fourqurean, J. W., C. M. Duarte, H. Kennedy, and others. 2012. Seagrass ecosystems as a globally significant carbon stock. Nat. Geosci. **5**: 505–509. doi:10.1038/ngeo1477

Gacia, E., and C. M. Duarte. 2001. Sediment retention by a Mediterranean Posidonia oceanica meadow: The balance between deposition and resuspension. Estuar. Coast. Shelf Sci. **52**: 505–514. doi:10.1006/ecss.2000.0753

Greiner, J. T., K. J. McGlathery, J. Gunnell, and B. A. McKee. 2013. Seagrass Restoration Enhances "Blue Carbon" Sequestration in Coastal Waters. PLoS One **8**: e72469. doi:10.1371/journal.pone.0072469

Hansen, J., and M. A. Reidenbach. 2013. Seasonal Growth and Senescence of a Zostera marina Seagrass Meadow Alters Wave-Dominated Flow and Sediment Suspension Within a Coastal Bay. Estuaries and Coasts **36**: 1099–1114. doi:10.1007/s12237-013-9620-5

Hasegawa, N., M. Hori, and H. Mukai. 2008. Seasonal changes in eelgrass functions: Current velocity reduction, prevention of sediment resuspension, and control of sediment-water column nutrient flux in relation to eelgrass dynamics. Hydrobiologia **596**: 387–399. doi:10.1007/s10750-007-9111-4

Johannessen, S. C., and R. W. Macdonald. 2016. Geoengineering with seagrasses: Is credit due where credit is given? Environ. Res. Lett. **11**: 113001. doi:10.1088/1748-9326/11/11/113001

Lawson, S. E., P. L. Wiberg, K. J. McGlathery, and D. C. Fugate. 2007. Wind-driven sediment suspension controls light availability in a shallow coastal lagoon. Estuaries and Coasts **30**: 102–112. doi:10.1007/BF02782971

Lesser, G. R., J. A. Roelvink, J. A. T. M. T. M. van Kester, and G. S. Stelling. 2004. Development and validation of a three-dimensional morphological model. Coast. Eng. **51**: 883–915. doi:10.1016/j.coastaleng.2004.07.014

Lin, Q., E. Liu, E. Zhang, R. Bindler, B. Nath, K. Zhang, and J. Shen. 2022. Spatial variation of organic carbon sequestration in large lakes and implications for carbon stock quantification. CATENA **208**: 105768. doi:10.1016/J.CATENA.2021.105768

McGlathery, K. J., L. K. Reynolds, L. W. Cole, R. J. Orth, S. R. Marion, and A. Schwarzschild. 2012. Recovery trajectories during state change from bare sediment to eelgrass dominance. Mar. Ecol. Prog. Ser. **448**: 209–221. doi:10.3354/meps09574

McGlathery, K., K. Sundbäck, and I. Anderson. 2007. Eutrophication in shallow coastal bays and lagoons: the role of plants in the coastal filter. Mar. Ecol. Prog. Ser. **348**: 1–18. doi:10.3354/meps07132

Moki, H., K. Taguchi, Y. Nakagawa, S. Montani, and T. Kuwae. 2020. Spatial and seasonal impacts of submerged aquatic vegetation (SAV) drag force on hydrodynamics in shallow waters. J. Mar. Syst. **209**: 103373. doi:10.1016/J.JMARSYS.2020.103373

Nardin, W., and D. A. Edmonds. 2014. Optimum vegetation height and density for inorganic sedimentation in deltaic marshes. Nat. Geosci. **7**: 722–726. doi:10.1038/NGEO2233

Nardin, W., L. Larsen, S. Fagherazzi, and P. Wiberg. 2018. Tradeoffs among hydrodynamics, sediment fluxes and vegetation community in the Virginia Coast Reserve, USA. Estuar. Coast. Shelf Sci. **210**: 98–108. doi:10.1016/j.ecss.2018.06.009

Nolte, S., E. C. Koppenaal, P. Esselink, K. S. Dijkema, M. Schuerch, A. V. De Groot, J. P. Bakker, and S. Temmerman. 2013. Measuring sedimentation in tidal marshes: A review on methods and their applicability in biogeomorphological studies. J. Coast. Conserv. **17**: 301–325. doi:10.1007/s11852-013-0238-3

Oliver, E. C. J., M. T. Burrows, M. G. Donat, and others. 2019. Projected Marine Heatwaves in the 21st Century and the Potential for Ecological Impact. Front. Mar. Sci. **6**: 734. doi:10.3389/fmars.2019.00734

Oreska, M. P. J., K. J. McGlathery, L. R. Aoki, A. C. Berger, P. Berg, and L. Mullins. 2020. The greenhouse gas offset potential from seagrass restoration. Sci. Rep. **10**: 1–15. doi:10.1038/s41598-020-64094-1

Oreska, M. P. J., K. J. McGlathery, and J. H. Porter. 2017. Seagrass blue carbon spatial patterns at the meadow-scale. PLoS One **12**: e0176630. doi:10.1371/journal.pone.0176630

Oreska, M. P. J., G. M. Wilkinson, K. J. McGlathery, M. Bost, and B. A. McKee. 2018. Non-seagrass carbon contributions to seagrass sediment blue carbon. Limnol. Oceanogr. **63**: S3–S18. doi:10.1002/lno.10718

Orth, R. J., T. J. B. Carruthers, W. C. Dennison, and others. 2006. A Global Crisis for Seagrass Ecosystems. Bioscience **56**: 987–996. doi:10.1641/0006-3568(2006)56[987:AGCFSE]2.0.CO;2

Pendleton, L., D. C. Donato, B. C. Murray, and others. 2012. Estimating Global "Blue Carbon" Emissions from Conversion and Degradation of Vegetated Coastal Ecosystems. PLoS One **7**: e43542. doi:10.1371/journal.pone.0043542

Potouroglou, M., J. C. Bull, K. W. Krauss, and others. 2017. Measuring the role of seagrasses in regulating sediment surface elevation. Sci. Rep. **7**: 1–11. doi:10.1038/s41598-017-12354-y

Reidenbach, M. A., and E. L. Thomas. 2018. Influence of the Seagrass, Zostera marina, on Wave Attenuation and Bed Shear Stress Within a Shallow Coastal Bay. Front. Mar. Sci. **5**: 397. doi:10.3389/fmars.2018.00397

Rheuban, J. E., P. Berg, and K. J. McGlathery. 2014. Ecosystem metabolism along a colonization gradient of eelgrass (*Zostera marina*) measured by eddy correlation. Limnol. Oceanogr. **59**: 1376–1387. doi:10.4319/lo.2014.59.4.1376

Ricart, A. M., P. H. York, M. A. Rasheed, M. Pérez, J. Romero, C. V. Bryant, and P. I. Macreadie. 2015. Variability of sedimentary organic carbon in patchy seagrass landscapes. Mar. Pollut. Bull. **100**: 476–482. doi:10.1016/j.marpolbul.2015.09.032

Samper-Villarreal, J., C. E. Lovelock, M. I. Saunders, C. Roelfsema, and P. J. Mumby. 2016. Organic carbon in seagrass sediments is influenced by seagrass canopy complexity, turbidity, wave height, and water depth. Limnol. Oceanogr. **61**: 938–952. doi:10.1002/LNO.10262

Sohma, A., H. Shibuki, F. Nakajima, A. Kubo, and T. Kuwae. 2018. Modeling a coastal ecosystem to estimate climate change mitigation and a model demonstration in Tokyo Bay. Ecol. Modell. **384**: 261–289. doi:10.1016/J.ECOLMODEL.2018.04.019

Suzuki, T., M. Zijlema, B. Burger, M. C. Meijer, and S. Narayan. 2012. Wave dissipation by vegetation with layer schematization in SWAN. Coast. Eng. **59**: 64–71. doi:10.1016/j.coastaleng.2011.07.006

Walter, R. K., J. K. O'Leary, S. Vitousek, M. Taherkhani, C. Geraghty, and A. Kitajima. 2020. Large-scale erosion driven by intertidal eelgrass loss in an estuarine environment. Estuar. Coast. Shelf Sci. **243**: 106910. doi:10.1016/j.ecss.2020.106910

Waycott, M., C. M. Duarte, T. J. B. Carruthers, and others. 2009. Accelerating loss of seagrasses across the globe threatens coastal ecosystems. Proc. Natl. Acad. Sci. U. S. A. **106**: 12377–12381. doi:10.1073/pnas.0905620106

Wiberg, P. L., J. A. Carr, I. Safak, and A. Anutaliya. 2015. Quantifying the distribution and influence of non-uniform bed properties in shallow coastal bays. Limnol. Oceanogr. Methods **13**: 746–762. doi:10.1002/lom3.10063

Willmott, C. J. 1981. On the validation of models. Phys. Geogr. **2**: 184–194. doi:10.1080/02723646.1981.10642213

Wilson, K. L., and H. K. Lotze. 2019. Climate change projections reveal range shifts of eelgrass Zostera marina in the Northwest Atlantic. Mar. Ecol. Prog. Ser. **620**: 47–62. doi:10.3354/meps12973

Zhu, Q., P. L. Wiberg, and M. A. Reidenbach. 2021. Quantifying Seasonal Seagrass Effects on Flow and Sediment Dynamics in a Back-Barrier Bay. J. Geophys. Res. Ocean. **126**: e2020JC016547. doi:10.1029/2020JC016547

Acknowledgements

Primary support for this work was provided by the National Science Foundation (NSF) through the VCR LTER award 1832221 and Coastal SEES award 1427282. The developers of Delft3D are acknowledged for open access to their code. The authors thank Matthew P. J. Oreska for providing sediment organic carbon concentration and sand fraction data at the study site.

Conflict of Interest

None declared.

Figure Legends

Fig. 1 (a) Aerial image of the study area, (b) Model grid and bathymetry in South Bay, and (c) Typical monthly seagrass shoot density (*N*) at the central meadow throughout the year. Red dashed lines in (b) represent boundaries of three seagrass density classes (*N*, 0.8*N*, and 0.6*N*) used in the model (Table S1). The seagrass shoot density data shown in (c) were compiled from previous seasonal seagrass observations in South Bay (Hansen and Reidenbach 2013; Rheuban et al. 2014; Reidenbach and Thomas 2018; Berger et al. 2020).

Fig. 2 (a) Bed shear stress, (b) Total suspended sediment concentration (SSC), (c) Sediment accumulation rates, and (d) Organic carbon accumulation rates as a function of seagrass density, (e) Bar plots of seagrass density and changes of sediment accumulation rate in seagrass meadows under normal-density conditions (blue), lower-than-average winter density scenario (red), and higher-than-average winter density scenario (gray), and (f) Bar plots of seagrass density and changes of sediment accumulation rate in seagrass meadows under normal-density conditions and summer marine heatwave scenario (yellow). Red symbols in (c) and (d) are model results output from low-density scenarios using a seagrass shoot density of 0, 25, and 50 shoots m^{-2}, respectively. Details about model settings and seagrass characteristics used in model simulations are provided in Table S1.

Fig. 3 Relationship between modeled surface sediment organic carbon (C_{org}) accumulation rate and modeled sediment accumulation rate averaged across the meadow.

Fig. 4 Average seasonal sediment accumulation rates output from model simulations with typical seasonal seagrass characteristics: (a) summer growth and mid-season loss, (b) autumn regrowth, (c) winter senescence, and (d) early growth. (e) Box plots of cumulative sediment accumulation during summer growth and mid-season loss (SG) and winter senescence (WS) as a function of distance to the meadow edge. The black line in (a)-(d) shows the meadow outline. The data shown in (e) were extracted from 28 interior transects perpendicular to the northern, western, and southern edges of the meadow.

Fig. 5 Annual sediment erosion and deposition patterns (a) without seagrass effects and (b) with seagrass effects, (c) Water depth of the meadow, and (d) Histogram of modeled annual sediment accumulation rates within the meadow. The asterisk and triangle in (b) show locations of sediment cores for ^{210}Pb dating collected by Oreska et al. (2018) and Greiner et al. (2013), respectively. The red line in (d) represents the mean modeled sediment accumulation rate, while the black dashed line shows the average sediment accumulation rate by ^{210}Pb dating.

Fig. 6 Box plots of annual sediment erosion/deposition within seagrass meadows as a function of depth without seagrass effects (a) and with seagrass effects (b).

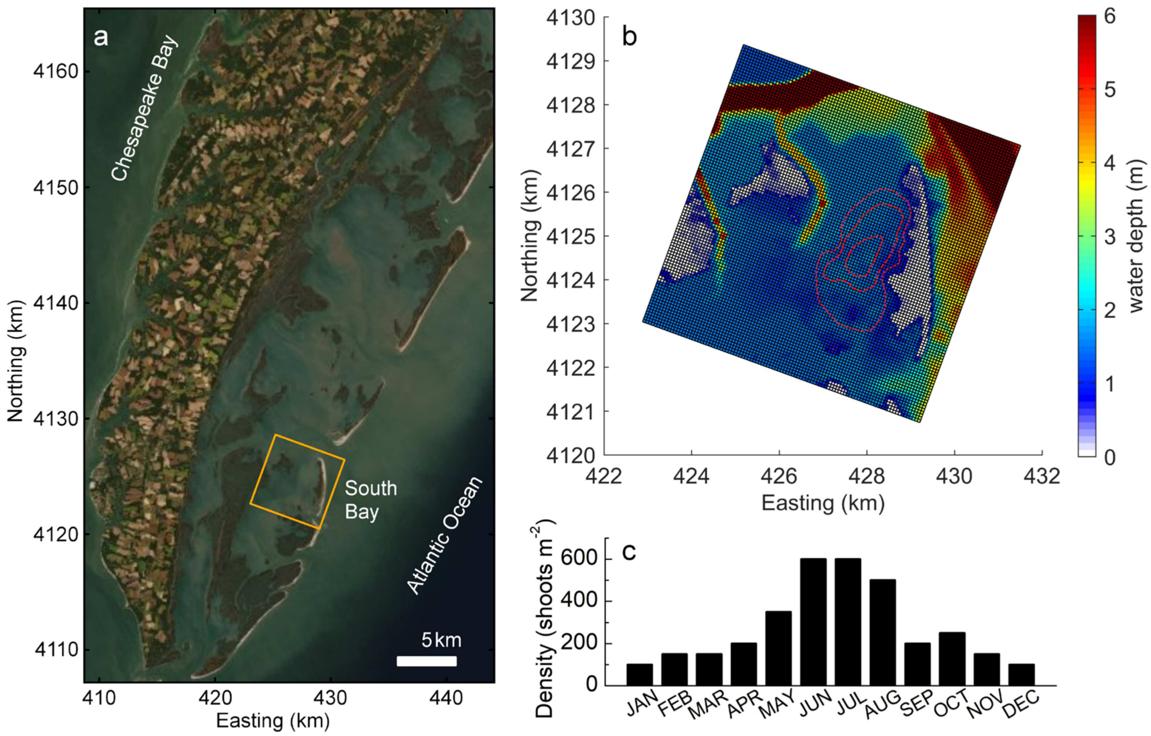
a
Chesapeake Bay
South Bay
Atlantic Ocean
5km
Northing (km)
Easting (km)
b
water depth (m)
Northing (km)
Easting (km)
c
Density (shoots m^{-2})
JAN
FEB
MAR
APR
MAY
JUN
JUL
AUG
SEP
OCT
NOV
DEC

Fig. 1

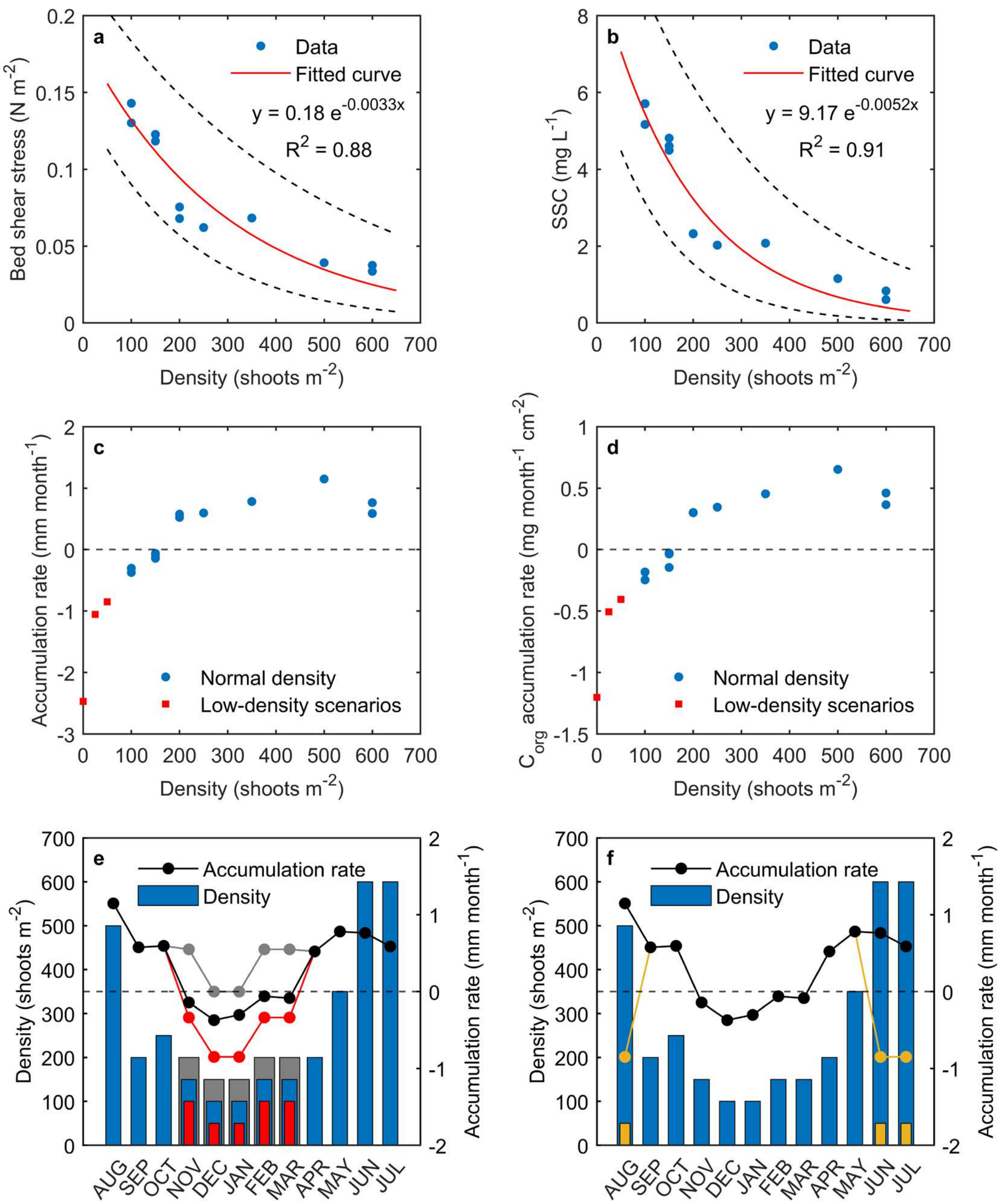
a
Data
Fitted curve
y = 0.18 e^-0.0033x
R^2 = 0.88
Bed shear stress (N m^-2)
Density (shoots m^-2)
b
Data
Fitted curve
y = 9.17 e^-0.0052x
R^2 = 0.91
SSC (mg L^-1)
Density (shoots m^-2)
c
Normal density
Low-density scenarios
Accumulation rate (mm month^-1)
Density (shoots m^-2)
d
Normal density
Low-density scenarios
C_org accumulation rate (mg month^-1 cm^-2)
Density (shoots m^-2)
e
Accumulation rate
Density
Density (shoots m^-2)
Accumulation rate (mm month^-1)
AUG SEP OCT NOV DEC JAN FEB MAR APR MAY JUN JUL
f
Accumulation rate
Density
Density (shoots m^-2)
Accumulation rate (mm month^-1)
AUG SEP OCT NOV DEC JAN FEB MAR APR MAY JUN JUL

Fig. 2

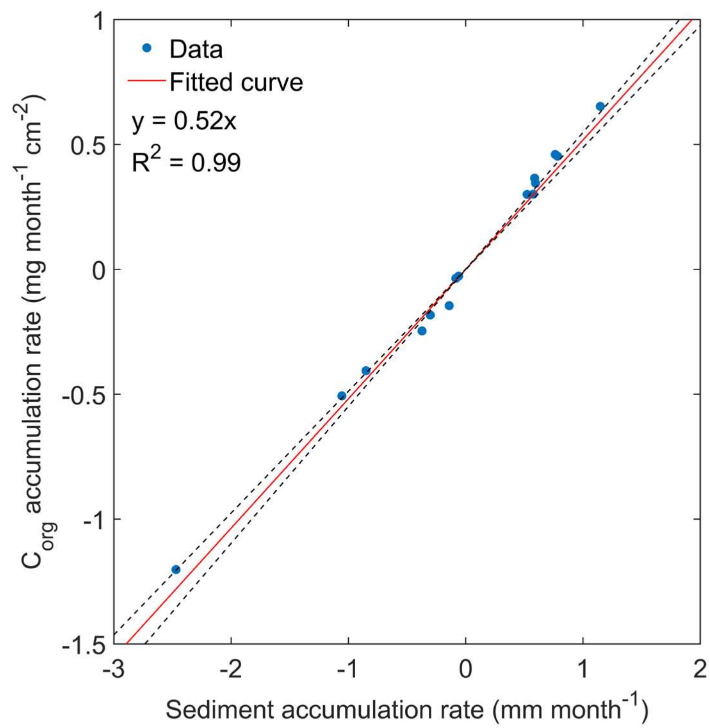
Data
Fitted curve
y = 0.52x
R2 = 0.99
Corg accumulation rate (mg month-1 cm-2)
Sediment accumulation rate (mm month-1)
1
0.5
0
-0.5
-1
-1.5
-3
-2
-1
0
1
2

Fig. 3

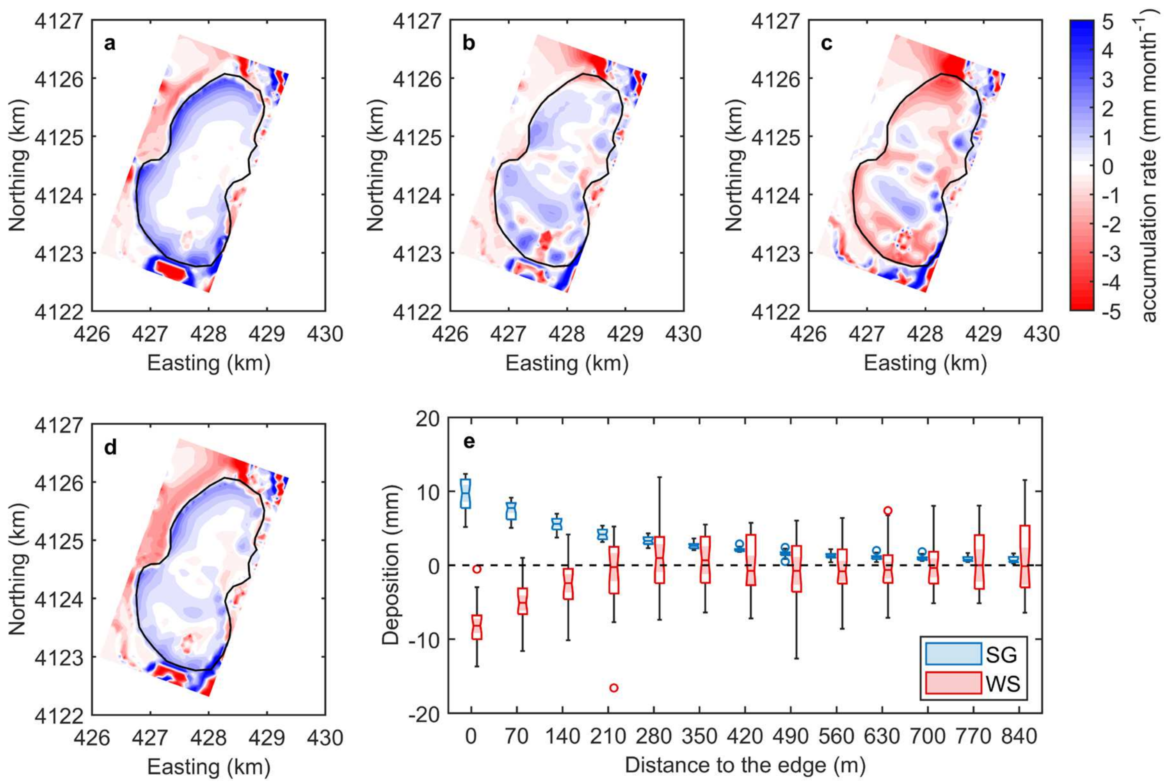
a
b
c
d
e
4127
4126
4125
4124
4123
4122
426
427
428
429
430
Northing (km)
Easting (km)
accumulation rate (mm month^{-1})
5
4
3
2
1
0
-1
-2
-3
-4
-5
Deposition (mm)
20
10
0
-10
-20
0 70 140 210 280 350 420 490 560 630 700 770 840
Distance to the edge (m)
SG
WS

Fig. 4

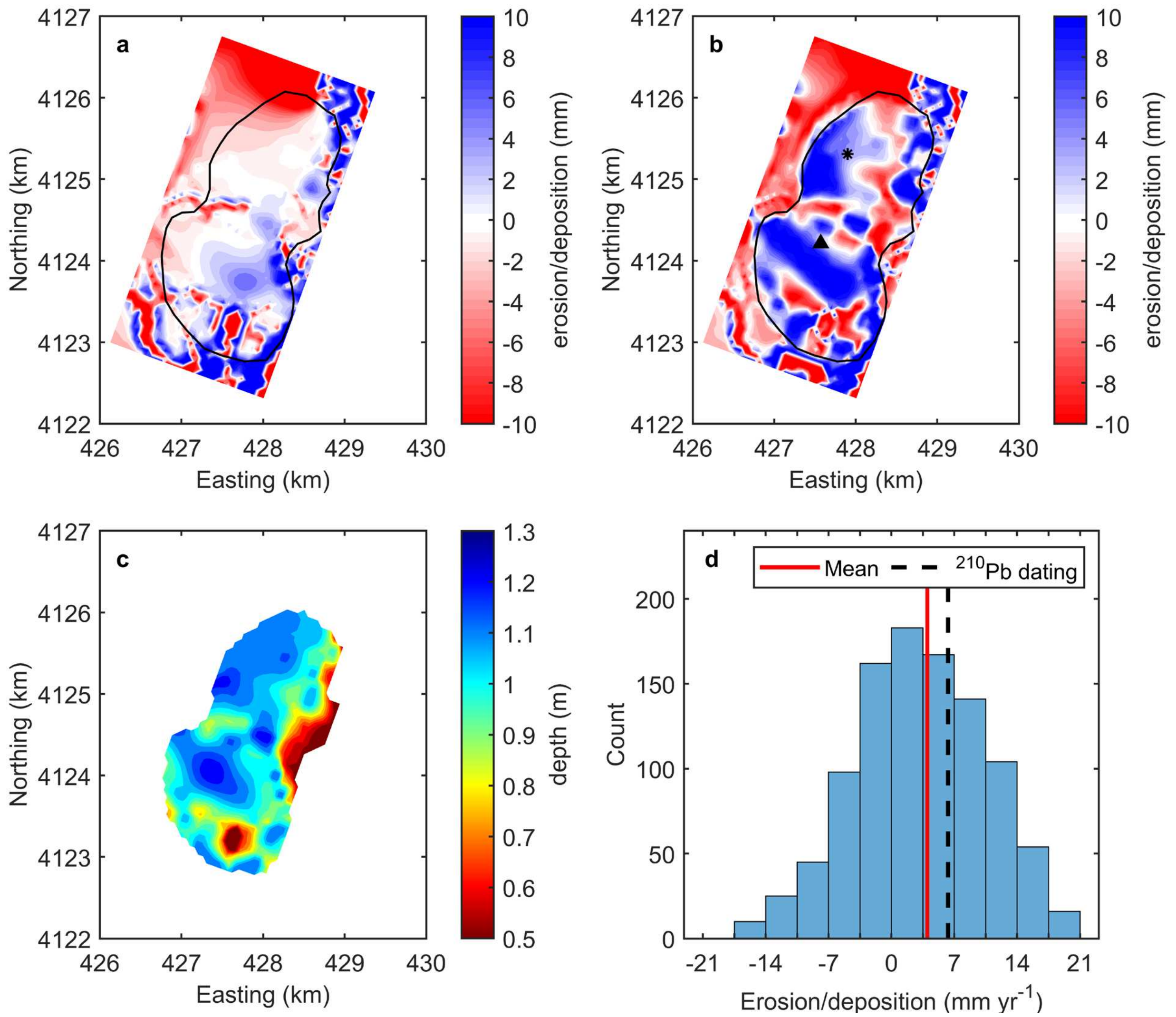
a
b
c
d
Northing (km)
Easting (km)
erosion/deposition (mm)
depth (m)
Mean
^{210}Pb dating
Count
Erosion/deposition (mm yr^{-1})

Fig. 5

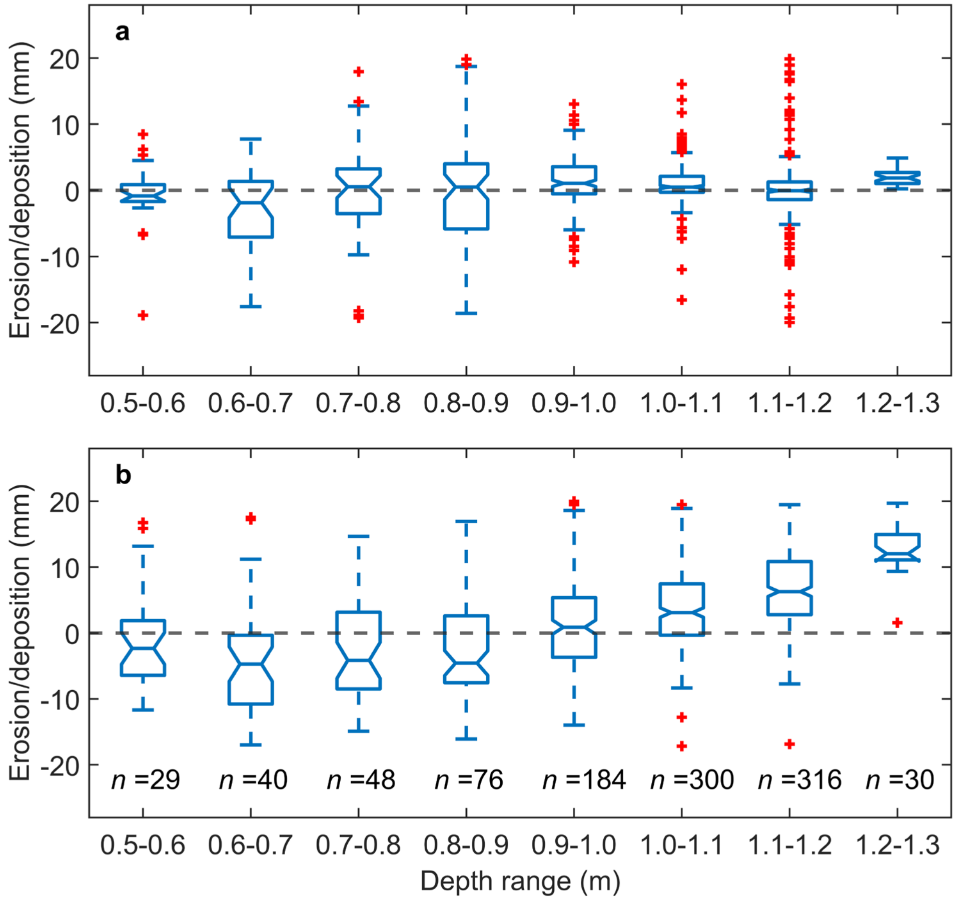

a
b
Erosion/deposition (mm)
20
10
0
-10
-20
n =29
n =40
n =48
n =76
n =184
n =300
n =316
n =30
0.5-0.6
0.6-0.7
0.7-0.8
0.8-0.9
0.9-1.0
1.0-1.1
1.1-1.2
1.2-1.3
Depth range (m)

596

597 Fig. 6